

Determination of superconducting anisotropy from magnetization data on random powders as applied to $\text{LuNi}_2\text{B}_2\text{C}$, $\text{YNi}_2\text{B}_2\text{C}$ and MgB_2 .

S. L. Bud'ko, V. G. Kogan, and P. C. Canfield

Ames Laboratory and Department of Physics and Astronomy, Iowa State University, Ames, Iowa

50011

(November 21, 2018)

Abstract

The recently discovered intermetallic superconductor MgB_2 appears to have a highly anisotropic upper critical field with $H_{c2}^{\max}/H_{c2}^{\min} \equiv \gamma > 5$. In order to determine the temperature dependence of both H_{c2}^{\max} and H_{c2}^{\min} we propose a method of extracting the superconducting anisotropy from the magnetization $M(H, T)$ of randomly oriented powder samples. The method is based on two features in $(\partial M/\partial T)_H$: the onset of diamagnetism at T_c^{\max} , that is commonly associated with H_{c2} , and a kink in $\partial M/\partial T$ at a lower temperature T_c^{\min} . Results for $\text{LuNi}_2\text{B}_2\text{C}$ and $\text{YNi}_2\text{B}_2\text{C}$ powders are in agreement with anisotropic H_{c2} obtained from magneto-transport measurements on single crystals. Using this method on four different types of MgB_2 powder samples we are able to determine $H_{c2}^{\max}(T)$ and $H_{c2}^{\min}(T)$ with $\gamma \approx 6$.

74.25.Dw, 74.60.Ec, 74.25.Ha

Typeset using REVTeX

Anisotropic type-II superconductors have been studied for a number of years¹ with a revisited interest after the discovery of strongly anisotropic high- T_c cuprates. The possibility has recently been raised that MgB_2 ($T_c \approx 40$ K) may also be highly anisotropic.² The quantitative characterisation of the anisotropy is usually one of the first questions to be addressed after the material is synthesized. One of the most accurate methods of extracting the anisotropy parameter $\gamma = H_{c2}^{\max}/H_{c2}^{\min}$ is by measuring the torque upon the single crystal sample in intermediate fields $H_{c1} \ll H \ll H_{c2}$ inclined relative to the crystal axes (we are interested here in uniaxial materials with large Ginzburg-Landau (GL) parameter $\kappa = \lambda/\xi$; λ and ξ are the penetration depth and the coherence length, H_{c1} and H_{c2} are the lower and the upper critical fields).³ The method is based on the existence of the transverse magnetization in anisotropic superconductors which causes the torque, the angular dependence of which depends only on γ .⁴

Often, materials are first synthesized in a polycrystalline form. Anisotropy estimates of such samples can be inferred by a number of measurements. In one of the common schemes,⁵ a powder of the material is mixed with a low magnetic background epoxy and aligned in a high magnetic field. The alignment is made permanent by curing the epoxy. The necessary requirements include a powder that consists of single crystalline grains with a considerable normal state magnetic anisotropy. The samples obtained in this way are suitable for anisotropic magnetization measurements. Usually, uncertainties in a degree of alignment lead to underestimates of γ .

We describe here a simple method to assess the anisotropy and to delineate $H_{c2}^{\max}(T)$ and $H_{c2}^{\min}(T)$ by analysis of the magnetization $M(T)$ taken for several values of the applied field H . We establish the validity of this method by comparison of anisotropic $H_{c2}(T)$ measured directly (by magneto-transport) on single crystals of quaternary borocarbide superconductors⁶ $\text{LuNi}_2\text{B}_2\text{C}$ and $\text{YNi}_2\text{B}_2\text{C}$ with the values extracted from the $M(H, T)$ data on randomly oriented powders. We then use the method to determine the curves of $H_{c2}^{\max}(T)$ and $H_{c2}^{\min}(T)$ for MgB_2 and to obtain $\gamma \approx 6$, close to the values given in Ref. 2.

Single crystals of $\text{LuNi}_2\text{B}_2\text{C}$ and $\text{YNi}_2\text{B}_2\text{C}$ were grown using the Ni_2B flux growth

technique.^{6,7} Four different samples of MgB_2 were used in this work: (i) polycrystalline sintered Mg^{11}B_2 , (ii) MgB_2 wire segments, and commercial 99.5% purity MgB_2 powders from two sources: (iii) Accumet Materials Co. and (iv) Alfa Aesar. Samples (i) and (ii) were synthesized by reacting elemental boron with Mg at 950°C .^{8–10}

The anisotropic $H_{c2}(T)$ of $\text{LuNi}_2\text{B}_2\text{C}$ and $\text{YNi}_2\text{B}_2\text{C}$ single crystals were measured directly by monitoring resistance $R(H, T)$ near the superconducting transition. For the magnetization measurements, single crystals of borocarbides and bulk samples of MgB_2 were ground to powder, mixed with Epocast 121 epoxy (the epoxy has weak featureless diamagnetism in the $H - T$ range of interest), stirred to assure random orientation of particles and cured at 120°C for 1 hour. DC magnetization measurements were performed in Quantum Design MPMS-5 or MPMS-7 SQUID magnetometers. Resistance of borocarbides were measured using LR-700 AC resistance bridge ($f = 16\text{ Hz}$, $I = 1\text{--}3\text{ mA}$) and the $H - T$ environment of the MPMS instruments. Contacts to the samples were made with Epo-tek H20E silver epoxy. Currents were flowing in the ab plane, whereas the field was applied perpendicular to the current, along c axis or in the ab plane.

The data on anisotropic H_{c2} for non-magnetic borocarbides were reported in several publications.^{11–14} Since the H_{c2} anisotropy appears to be somewhat sample-dependent, we performed direct magneto-transport measurements on samples from the same batches that were used for random powder magnetization measurements. Figure 1 shows representative resistance, $R(H)$, data for $\text{LuNi}_2\text{B}_2\text{C}$ measured at constant temperatures for two field orientations. The resistively measured superconducting transition broadens slightly in field; this results in criterion-dependent $H_{c2}(T)$ curves. Still, the anisotropy of $H_{c2}(T)$ turns out practically criterion-independent. In the following we use the criterion of the maximum slope intersection with the $R = 0$ line, as shown in Fig.1.

An example of magnetization data, $M(T)$, in a constant field, $H = 30\text{ kG}$, for a powder sample of $\text{LuNi}_2\text{B}_2\text{C}$ is shown in Fig. 2 along with the temperature derivative $\partial M/\partial T$. We interpret the behavior of $\partial M/\partial T$ as follows. Upon cooling a powdered sample in a fixed H , there is a deviation from a roughly T independent normal state magnetization

(for non-magnetic materials as is the case for the three compounds discussed here) to an increasingly diamagnetic signal at $T = T_c^{max}$. A second sharp feature will occur in $\partial M/\partial T$ when the sample temperature passes through T_c^{min} . This can be most clearly understood by considering what happens to the sample upon warming. For $T < T_c^{min}$ all grains are superconducting whereas for $T > T_c^{min}$ part of them will become normal, depending upon their orientation with respect to the applied magnetic field. Therefore, upon warming through T_c^{min} there will be a kink in $\partial M/\partial T$ associated with the onset of normal state properties in an increasing number of appropriately oriented grains. In Fig. 2 this can be seen in the $\partial M/\partial T$ plot with $T_c^{max} = 10.6$ K and $T_c^{min} = 8.7$ K. The temperatures T_c^{min} and T_c^{max} are marked with vertical arrows in Fig. 2. It is worth noting that when a single $H_{c2}(T)$ value is obtained from measurements on polycrystalline samples it is actually the maximum upper critical field $H_{c2}^{max}(T)$.⁹

The $M(T)$ data taken for a number of fixed fields were analyzed in a similar manner; the resulting curves $H_{c2}^{min}(T)$ and $H_{c2}^{max}(T)$ are presented in the upper panel of Fig. 4 (open symbols). These are plotted together with the directly measured anisotropic $H_{c2}(T)$ from magneto-transport measurements on $\text{LuNi}_2\text{B}_2\text{C}$ single crystals from the same batch. It is seen that both sets of data are in agreement. We obtain $\gamma \approx 1.2 - 1.3$. Albeit slightly higher, this value of γ is consistent with values reported in literature: e.g. $\gamma \approx 1.2$.¹⁴ Similar measurements and analysis were performed on $\text{YNi}_2\text{B}_2\text{C}$. The results are shown in lower panel of Fig. 4. The slightly higher mismatch between the magneto-transport H_{c2} 's of single crystals and those extracted from powder magnetization measurements than for the case of $\text{LuNi}_2\text{B}_2\text{C}$ might be due to arbitrary in-plane field orientation in magneto-transport measurements, choice of criteria and/or error bars in the measurements.

It is worth noting that the method of extracting the anisotropic $H_{c2}(T)$ and the anisotropy parameter γ from the powder data presented here constitutes a robust procedure independent of a particular model for describing the anisotropy. Moreover, the method is just based on the existence of a kink in $\partial M/\partial T$ located at $T = T_c^{min}$, a feature which should be present for any angular distribution of the grains (as long as it is continuous, but

not necessarily random). The analysis of the $M(H, T)$ data can be pushed further to relate γ to other material characteristics (κ , λ , etc).^{21,22} This, however, would have involved more information (e.g., randomness, assumptions on linear dependences of M on $H_{c2} - H$ and $T_c - T$) and we will not pursue this here.

With the validity of this method established for borocarbides, we can use it for MgB_2 .²³ An example of magnetization curves for two values of H and their temperature derivatives are shown in Fig. 5. As in borocarbides, a clear feature at T_c^{min} is seen in $\partial M/\partial T$. With increasing H , this feature moves down in temperature faster than T_c^{max} and disappears for $H > 25$ kG.

$H_{c2}^{min}(T)$ and $H_{c2}^{max}(T)$ curves were deduced from magnetization data collected in fixed fields for four different samples of MgB_2 . These data are presented in Fig. 6. Data for the sintered powder and the powdered wire segments are very similar. The $H_{c2}^{max}(T)$ curves are consistent with the reported^{9,10} polycrystalline magneto-transport $H_{c2}(T)$. The extracted anisotropy is $\gamma \approx 5 - 6$. Both commercial MgB_2 powders have T_c values that are 1-1.5 K lower than sintered powder or wire segments (see Fig. 6), presumably due to a higher levels of impurities. The features in $\partial M/\partial T$ are less pronounced in commercial powders, however the resulting anisotropies are similar to that observed in clean MgB_2 (Fig. 6). For these samples $\gamma \approx 6 - 7$.

There have been some initial reports of the H_{c2} anisotropy for MgB_2 . The anisotropy γ for separate particles settled on a flat surface is 1.73.¹⁵ For a hot-pressed bulk sample, $\gamma \approx 1.1$.¹⁶ Measurements on c -axis oriented thin films¹⁷ gave $\gamma = 1.8 - 2$, with the higher γ for films with higher resistivity and lower T_c . Recently, there were several announcements on growth and anisotropic properties of sub-mm sized single crystals of MgB_2 .¹⁸⁻²⁰ In all three cases the residual resistance ratio was 5 - 7 and the transition temperature was $\approx 0.5 - 1$ K lower than for polycrystalline materials.^{8,10,23} The H_{c2} anisotropy was found to be in the range 2.6 - 3. A significantly higher H_{c2} anisotropy ($\gamma \approx 6 - 9$) was inferred from conduction electron spin resonance measurements and from fits to the reversible part of $M(H)$ on high purity and high residual resistance ratio samples². The results for MgB_2 obtained in this

work are consistent with the latter and are at the higher end of the wide-spread of values in the literature.

The method of extracting the superconducting anisotropy suggested in this paper works well for random powders of $\text{LuNi}_2\text{B}_2\text{C}$ and $\text{YNi}_2\text{B}_2\text{C}$, for which the results were compared with direct measurements of H_{c2} . Moreover, the γ values so obtained are in agreement with the microscopic theory²⁴ according to which

$$\gamma^2 = \frac{\langle \Delta(\mathbf{k}_F) v_{ab}^2 \rangle}{\langle \Delta(\mathbf{k}_F) v_c^2 \rangle}, \quad (1)$$

where v_i are the Fermi velocities and $\langle \dots \rangle$ stand for Fermi surface averages. For the isotropic gap function $\Delta(\mathbf{k}_F) = \text{constant}$, the band structure estimates give:^{25,26}

$$\gamma = \sqrt{\langle v_{ab}^2 \rangle / \langle v_c^2 \rangle} \approx 1.2. \quad (2)$$

This, however, is not the case for MgB_2 . The ratio $\langle v_{ab}^2 \rangle / \langle v_c^2 \rangle$ averaged over the *whole* Fermi surface for this material is close to unity,²⁷ whereas our values of γ^2 are in the range 25 – 50. This is indicative of a strong anisotropy of $\Delta(\mathbf{k}_F)$. There are arguments²⁸ that the electron-phonon interaction is particularly strong on the Fermi surface sheets shaped as slightly distorted cylinders along the c crystal direction. The ratio $\langle v_{ab}^2 \rangle / \langle v_c^2 \rangle$ averaged only over these cylinders is estimated as ≈ 40 .²⁹ If the gap Δ on the remaining Fermi surface sheets is negligible, we expect the superconducting anisotropy as $\gamma \approx \sqrt{40} \approx 6$, the value close to that extracted from our analysis of the magnetization.

In conclusion, we suggest a simple method of evaluation of the anisotropy of the upper critical field from the analysis of the temperature dependent magnetization of randomly oriented powders. In the case of non-magnetic borocarbides the results are in good agreement with the direct measurements on single crystals and with the band-structure calculations provided the gap is isotropic. For MgB_2 the estimated anisotropy is $\gamma \approx 5 - 7$, which can be reconciled with the band calculations only if the superconducting gap on the cylindrically shaped sheets of the Fermi surface is dominant.

We thank K. D. Belashchenko and V. P. Antropov for discussions and for providing the $\langle v_{ab}^2 \rangle / \langle v_c^2 \rangle$ value for cylindrical parts of MgB₂ Fermi surface. Ames Laboratory is operated for the U. S. Department of Energy by Iowa State University under contract No. W-7405-ENG-82. This work was supported by the Director of Energy Research, Office of Basic Energy Sciences.

REFERENCES

- ¹ R. C. Morris, R. V. Coleman, and R. Bhandari, Phys. Rev. B **5**, 895 (1972).
- ² F. Simon *et al.*, cond-mat/0104557, Phys. Rev. Lett., in press.
- ³ D. E. Farrell *et al.*, Phys. Rev. Lett. **64**, 1573 (1990).
- ⁴ V. G. Kogan, Phys. Rev. B **38**, 7049 (1988).
- ⁵ D. E. Farrell *et al.*, Phys. Rev. B **36**, 4025 (1987).
- ⁶ For review see: P. C. Canfield, P. L. Gammel, and D. J. Bishop, Physics Today **51**, 40 (1998) and references therein.
- ⁷ M. Xu *et al.*, Physica C **227**, 321 (1994).
- ⁸ S. L. Bud'ko *et al.* Phys. Rev. Lett. **86**, 1877 (2001).
- ⁹ D. K. Finnemore *et al.*, Phys. Rev. Lett. **86**, 2420 (2001).
- ¹⁰ P. C. Canfield *et al.*, Phys. Rev. Lett. **86**, 2423 (2001).
- ¹¹ M. Xu *et al.*, Physica C **235-240**, 2533 (1994).
- ¹² E. Johnston-Halperin *et al.*, Phys. Rev. B **51**, 12852 (1995).
- ¹³ K. D. D. Rathnayaka *et al.*, Phys. Rev. B **55**, 8506 (1997).
- ¹⁴ V. Metlushko *et al.*, Phys. Rev. Lett. **79**, 1738 (1997).
- ¹⁵ O. F. de Lima *et al.*, Phys. Rev. Lett. **86**, 5974 (2001).
- ¹⁶ A. Handstein *et al.*, cond-mat/0103408.
- ¹⁷ S. Patnaik *et al.*, Supercond. Sci. Technol. **14**, 315 (2001).
- ¹⁸ M. Xu *et al.*, cond-mat/0105271.
- ¹⁹ C. U. Jung *et al.*, cond-mat/0105330.

- ²⁰ S. Lee *et al.*, cond-mat/0105545.
- ²¹ V.G. Kogan and J.R. Clem, Jap. J. Appl. Phys. **26**, 1159 (1988).
- ²² L. I. Glazman, A. E. Koshelev, and A. G. Lebed', Sov. Phys. JETP, **67**, 1235 (1988).
- ²³ J. Nagamatsu *et al.*, Nature **410**, 63 (2001).
- ²⁴ L. P. Gor'kov and T.K. Melik-Barkhudarov, Soviet Phys. JETP, **18**, 1031 (1964).
- ²⁵ V. G. Kogan *et al.*, Phys. Rev. B **55**, R8693 (1997).
- ²⁶ S. B. Dugdale *et al.*, Phys. Rev. Lett. **83**, 4824 (1999).
- ²⁷ J. Kortus *et al.*, Phys. Rev. Lett., **86**, 4656 (2001).
- ²⁸ A. Y. Liu, I. I. Mazin, and J. Kortus, cond-mat/0103570.
- ²⁹ K. D. Belashchenko, V. P. Antropov, private communication.

FIGURES

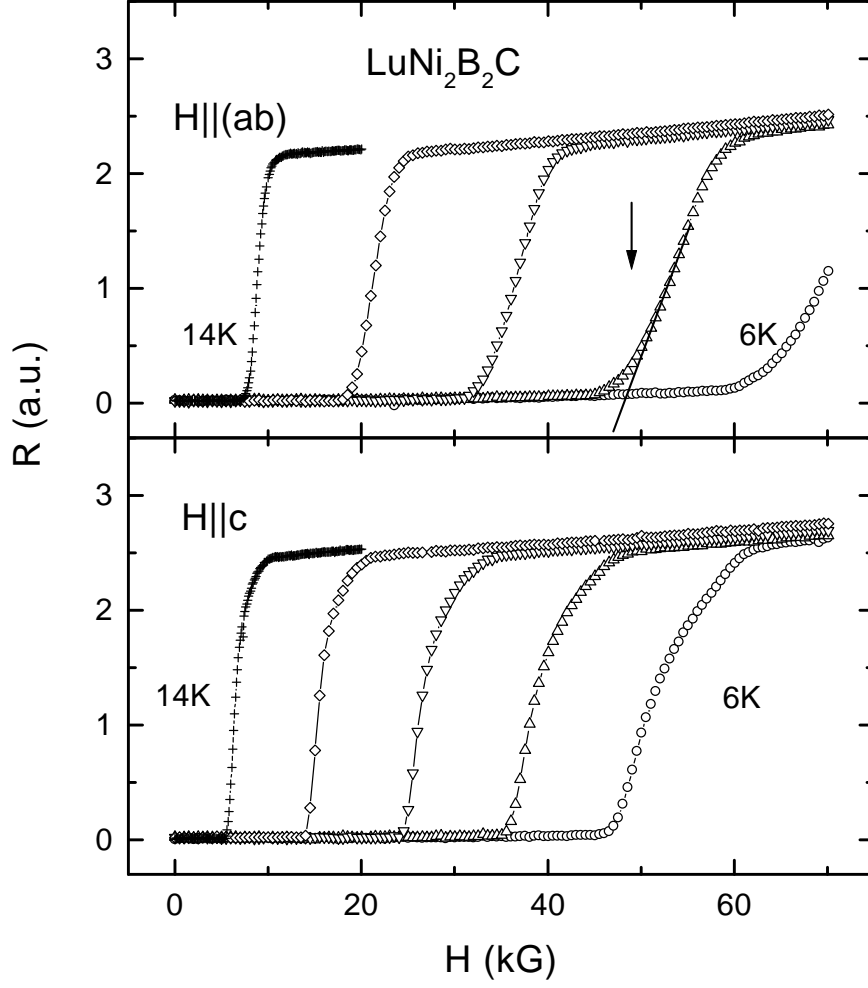


FIG. 1. Representative $R(H)$ curves for $\text{LuNi}_2\text{B}_2\text{C}$. Data shown are from 6 K to 14 K taken every 2 K. The criterion for $H_{c2}(T)$ is shown by the vertical arrow in the upper panel.

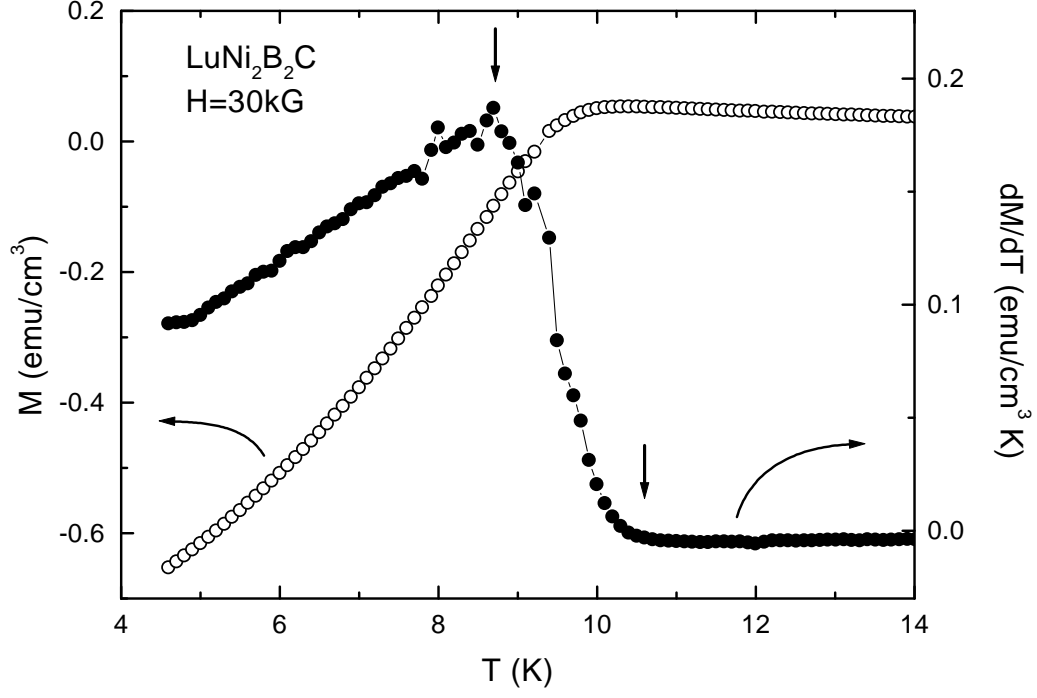


FIG. 2. Magnetization $M(T)$ for $H = 30$ kG and its temperature derivative for a randomly oriented powder of $\text{LuNi}_2\text{B}_2\text{C}$. The vertical arrows show $T_c^{\min}(H)$ and $T_c^{\max}(H)$.

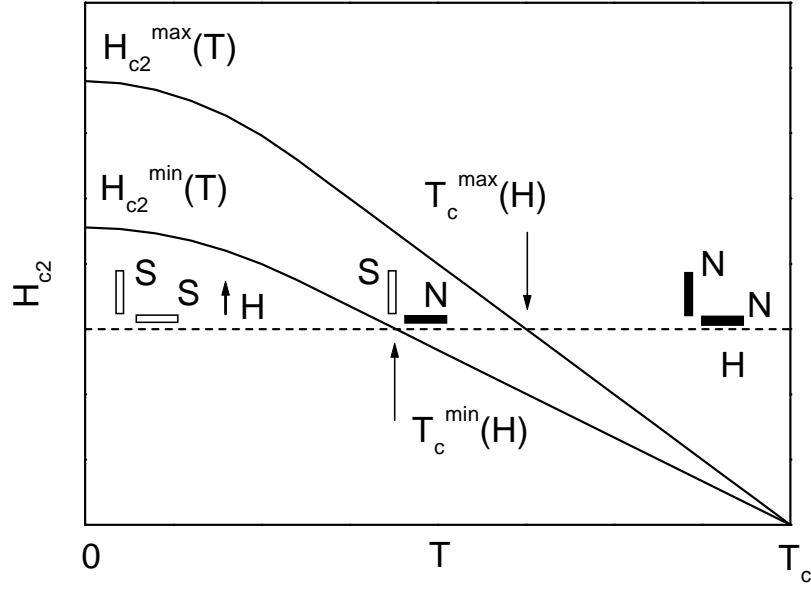


FIG. 3. Sketch of the maximum $H_{c2}^{max}(T)$ and the minimum $H_{c2}^{min}(T)$ upper critical fields. For a given applied field H , the relation $H = H_{c2}^{min}(T_c^{min}) = H_{c2}^{max}(T_c^{max})$ defines temperatures T_c^{min}, T_c^{max} . The open (shaded) rectangles represent superconducting (normal) grains for $T < T_c^{min}$, $T_c^{min} < T < T_c^{max}$, and $T > T_c^{max}$.

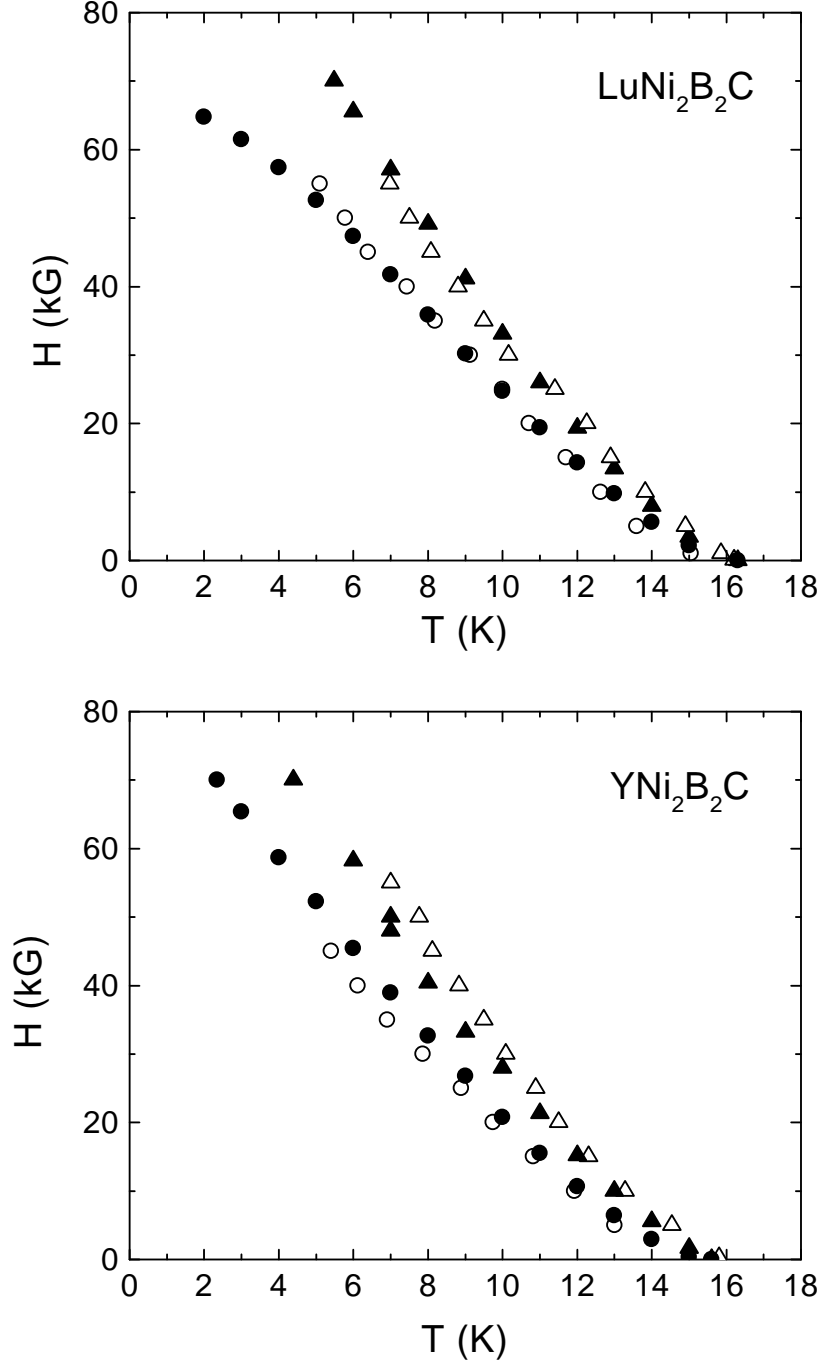


FIG. 4. The upper panel: the minimum upper critical field $H_{c2}^{\min}(T)$ (open circles) and the maximum one $H_{c2}^{\max}(T)$ (open triangles) for $\text{LuNi}_2\text{B}_2\text{C}$ powder obtained by analysis of $\partial M/\partial T$. Filled circles and triangles are $H_{c2}^c(T)$ and $H_{c2}^{ab}(T)$ respectively from magneto-resistance measurements on $\text{LuNi}_2\text{B}_2\text{C}$ crystals. The lower panel: the same for $\text{YNi}_2\text{B}_2\text{C}$

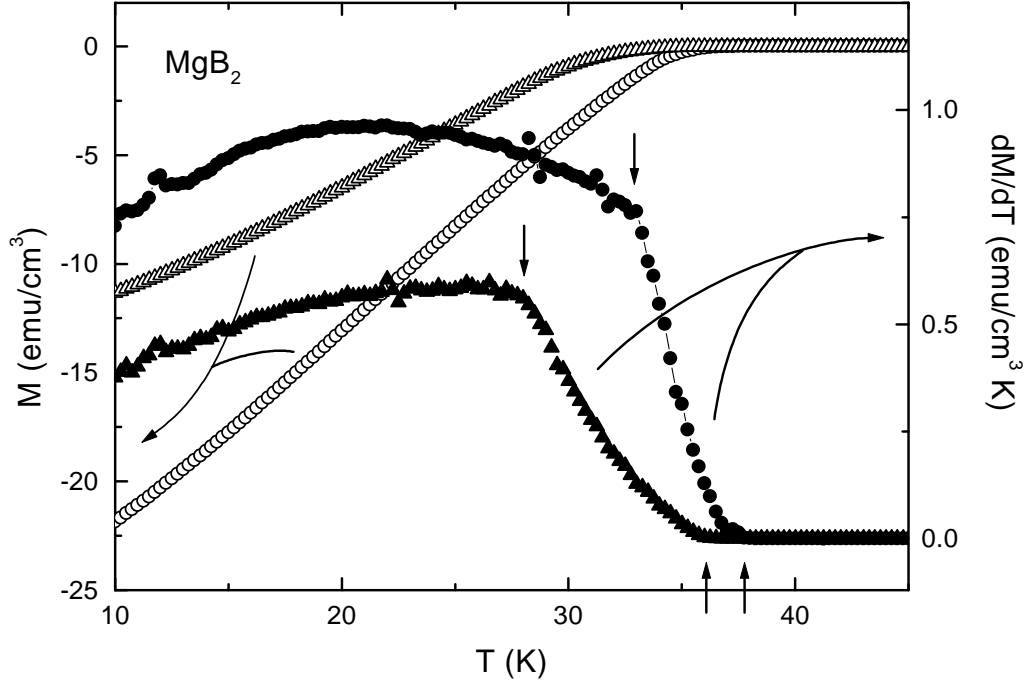


FIG. 5. Magnetization $M(T)$ of the powder sample of MgB_2 at $H = 5$ kG (open circles) and 10 kG (open triangles) and their temperature derivatives (respective filled symbols). The vertical arrows show $T_c^{\min}(H)$ and $T_c^{\max}(H)$ for each field.

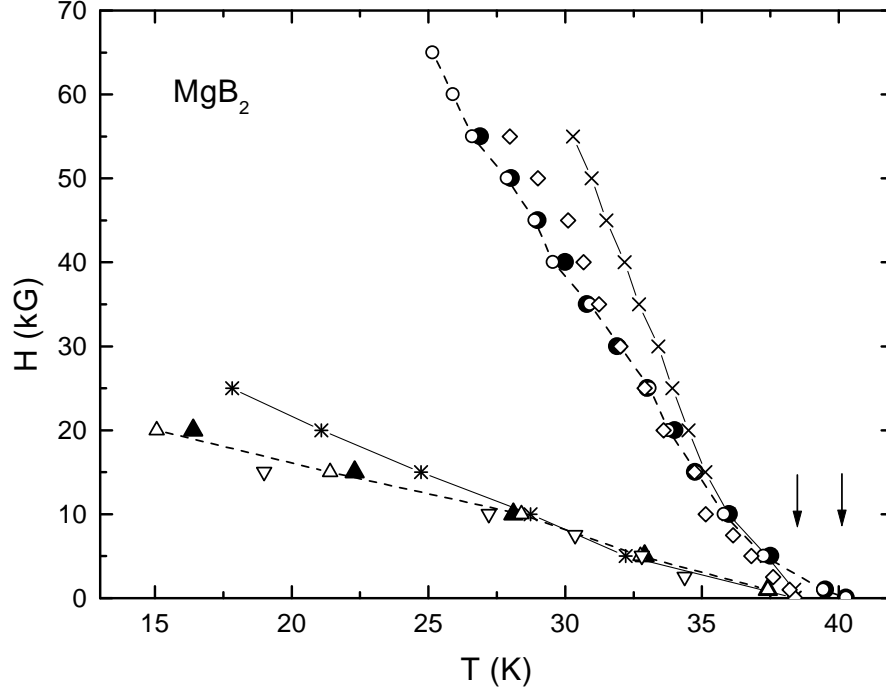


FIG. 6. Anisotropic $H_{c2}(T)$ curves for four different samples of MgB_2 obtained from the analysis of magnetization. Filled circles and up triangles - sintered powder, open circles and up triangles - wire segments, crosses and astericks - Accumet, open diamonds and down triangles - Alfa Aesar. The right vertical arrow shows T_c for sintered powder and wires, the left one, for commercial powders.